國立交通大學

電控工程研究所

碩士論文

於具有攻擊偵測機制之過程控制系統上論潛伏攻擊之影響

On Study of Stealthy Attacks in a Process Control System with Model-based Anomaly Detection Protection

研究生：黃啟彥

Student: Chi-Yen Huang

指導教授：黃育綸　博士

Advisor: Dr. Yu-Lun Huang

中華民國九十九年一月

January, 2010

於具有攻擊偵測機制之過程控制系統上論潛伏攻擊之影響

On Study of Stealthy Attacks in a Process Control System with Model-based Anomaly Detection Protection

研究生：黃啟彥　Student: Chi-Yen Huang

指導教授：黃育綸　博士　Advisor: Dr. Yu-Lun Huang

國立交通大學

電控工程研究所

碩士論文

A Thesis

Submitted to Institute of Electrical Control Engineering

College of Electrical Engineering

National Chiao Tung University

in partial Fulfill of the Requirements

for the Degree of

Master

in

Institute of Electrical Control Engineering

January, 2010

Hsinchu, Taiwan, Republic of China

中華民國九十九年一月

於具有攻擊偵測機制之過程控制系統上論潛伏攻擊之影響

學生：黃啟彥　　　　　　　　　　　　指導教授：黃育綸　博士

國立交通大學電控工程研究所碩士班

摘要

過程控制系統(PCS)具有穩定系統運作的能力，常被廣泛應用於現今的基礎建設及大型工廠中。由於這類系統的任何毀損都可能造成極重大的災難，並奪走數千條人命，因此2008年即有研究學者針對Tennessee-Eastman過程控制系統(TE-PCS)提出一套以模型為基礎的攻擊偵測模組(mADM)，確保TE-PCS能維持在穩定的工作範圍內。mADM利用真實訊號與內部模擬訊號的累計差值，來推斷系統的感測器是否遭人破壞，而對系統進行不利之攻擊。為保證PCS受到mADM的良好保護，在本篇論文中，我們以內賊的角度，對系統進行潛伏攻擊，以評估mADM之強健性。所謂內賊即為可能(1)熟知mADM的運作與參數或(2)擁有更改mADM參數權力之人；透過潛伏攻擊，可以在不被mADM偵測的情況下，使系統不當運作，而造成營運成本上升或工廠機具毀損。在分析mADM的設計後，我們依據累計差值的曲線變化，設計三種訊號曲線（凸面、斜線和凹面），以組成各種不同類型的潛伏攻擊，並進一步地攻擊以mADM保護之PCS。以TE-PCS為例，我們設計一系列的實驗，找出最有效的攻擊目標(感測器)和其相對應之攻擊方法。實驗結果證明當mADM參數落於安全範圍值時，潛伏攻擊無法造成系統崩解。但是，如果內賊擁有更改mADM參數的權力，則系統必須嚴加控管mADM參數的設定，否則過高的參數值會使系統遭受攻擊而損毀，過低的值則會使系統頻繁地發出錯誤警示，而增加營運成本。最後，我們演示三個例子，説明在不同的收支比下，潛伏攻擊

會使系統整體營利損失0.06%至41%。

On Study of Stealthy Attacks in a Process Control System with Model-based Anomaly Detection Protection

Student: Chi-Yen Huang Advisor: Dr. Yu-Lun Huang

Institute of Electrical Control Engineering

National Chiao Tung University

Abstract

Process control systems (PCS) are widely used in modern infrastructures and industrial plants for stabilizing safety-critical processes. Any disruption in such systems may cause serious human injuries and environmental disasters. In 2008, Lin et al. proposed a model-based anomaly detection module (abbreviated to mADM) to assure the security and stability of a well-studied Tennessee-Eastman process control system (TE-PCS). By taking advantages of cumulating the differences between real and simulated signals, mADM was able to detect an attack that compromises one or more sensors to crash the system. To evaluate the robustness of mADM, we study the stealthy attacks launched by an insider who may (1) know the detection and response strategies of mADM or (2) adjust the parameters of mADM so that these stealthy attacks may successfully attack the system without being detected by mADM. After analyzing mADM, we prove that a general stealthy attack signal can be represented by three types of curves, convex curve (cv), slope (sl), and concave curve (cc), depending on the cumulative differences of signals. By conducting a series of experiments on TE-PCS, we can identify the weakest sensor and the most effective way to stealthily attack this sensor. We also show that, if an insider cannot adjust the parameter settings and the parameters are well configured, he may not be able to crash the system. In the case that the insider obtains the permission to adjust the parameter settings, mADM should self-check whether the settings fall within valid ranges. Over-the-threshold settings may lead to a crash without being detected while under-the-threshold values may result in frequent false alarms and increase the operating costs. In the end, we also demonstrate three case studies to discuss that stealthy attacks may decrease the profits from 0.06% to 41%, depending on the ratio of costs and sales prices.

謝誌

猶如每位得獎者感言所述：「謝謝父母、家人給我的鼓勵與支持......」成就一件事物要謝天、謝地、謝東、謝西、謝南、謝北，要感謝的除了人，還有天地萬物，怎麼也謝不完。以下將以寥寥數字，重點感謝身邊的人事物，其未於文中提及者，便以陳之藩先生最常被引用的名句：「因為需要感謝的人太多了，就感謝天罷。」一併感謝之。

能夠完成此篇論文首先感謝余之業師 黃育綸博士，教授為我大學時代之導師，在學業上即有相當的提點，一路到研究所，更是教會我如何發現問題、研究問題、解決問題。也感謝老師參加iCAST (The International Collaboration for Advancing Security Technology)計劃，提供我赴美國加州柏克萊分校機會，接受Doug Tygar教授、Alvaro Cardenas、Saurabh Amin博士的提攜。另外感謝於柏克萊認識的朋友(特別是黃氏同宗的湘瑀大姊)，有你們的相互扶持，才得以讓我這隻身異鄉客有所依靠。

接下來此段落我們將討論實驗室室友對一研究生之影響。曾勁源學長:一表人才的大師兄，對人親切和藹，帶我去聯誼和我打桌球。蔡欣宜學姊:鄰座大師姊是遇到問題時的最佳求救對象，曾透過電扇聽我告解。黃詠文學長:從Sopca星球來，人人都欠他幾億，碰到技術上的困難，找他必解。鍾興龍學長:客家阿龍教我客語，帶我去爬仙山。張立穎學長:進lab時正逢學長準備畢業，讓我了解到報告的形式。陸培華學長:相處時間不長，但也是我入門時期的重要影響者。洪精佑學長:生動活潑的鵬兄，是我的菜。王鈺婷學姊:常常奮戰到天亮的summation，讓我知道什麼才叫做研究。甄元彬學長:有阿彬陪我遊山玩水，説衝就衝，實在難能可貴。許正道學長:道道正經的表面下，暗藏不少爆點。張宗堯學長:小狼常提供我諮商，是心靈上的好夥伴。陳柏廷學長:龜槍學長小叮噹，為一可敬的牌咖。林宗勳學長:基於帥動的東西，我才能順利走到今天。夏拉喬學姊:shylu親自下廚，引我品嚐新奇的印度口味。吳思穎同學:思思姊也是牌場上的

女中豪傑。王雅萱同學:多謝鄉鄉姊在美國的照應，莫名的笑點，引人苦笑。 彭博群同學:有讀書強迫症的澎哥，沉著穩重的個性收斂了我的性格。黃晉澤同學:從大學到研究所變了很多的睪哥，不失為一好玩伴。吳嘉稘學弟:愛嗆學長姊的稘稘，謝謝你沒冒犯我。 許鴻生學弟:超像Judo的Juju，取代wiper精實的臂膀。鄭偉強學弟:比我還好動的強強，展現了許多生活小智慧。黃錦銘學弟:有敏敏加入RTES，大家的啟笑聲分貝更是一天大過一天！ 黃奕奇學弟:先感謝你還沒寄來的賀年卡。葉書宏學弟:雖然酥酥還沒進來，相信你能挑起實驗室大樑的。賴鈺婷學妹:謝謝嗨嗨上回帶來的伴手禮。實驗室有以上所有人同進退地陪伴，或多或少影響著每日的生活，讓研究所生涯充滿歡笑，少了妳/你們，生活一定沒那麼多姿采。除此之外還有97級同學們、電控學長姊、學弟妹、電機學弟妹，認識妳/你們使我竊得認識王之名。最後還要感謝交大電機系壘，有你們，使我的休閒時光更精彩。在此以詩一首警惕自己莫忘吾師。

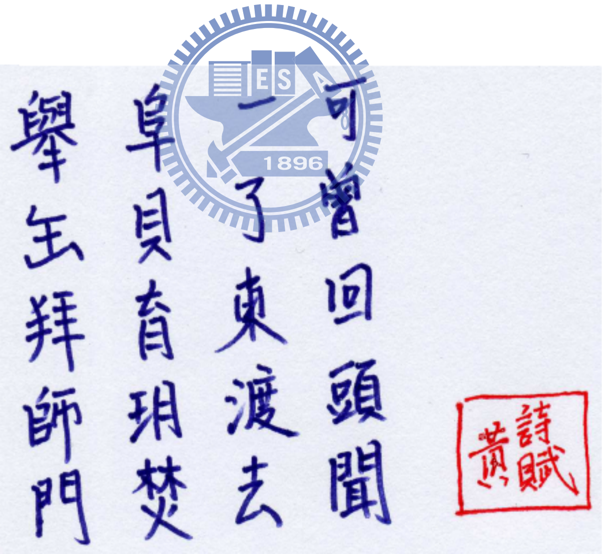

可曾回頭聞
一了東渡去
阜貝育玥焚
舉玉拜師門

詩賦黃

Figure 1: Key=717613121192

Contents

List of Figures

List of Tables

Chapter 1

Introduction

1.1 Motivation

Process control systems are capable of monitoring, computing, and managing to stabilize safety-critical processes [1] in infrastructures [2] and industrial plants. Process control systems are composed of a set of networked devices, such as sensors, actuators, controllers and communication devices [3], [4]. Recent researches have pointed out new vulnerabilities and threats in the process control systems [5], [6], [7], [8]. While most of the researches [9] and [10] utilize IT technologies to solve the cyber-security issues of process control systems, [5] discusses the differences between traditional IT security and process control system security.

Since process control systems are using in infrastructures and industrial plants, any disruption of these systems can cause serious damage to human lives. Fault diagnosis and fault-tolerant control enables systems to operate properly when a component failure occurs. The system isolates the detected failed component and reconfigures the control loop to ensure the proper operation. Sensors measurements compromised attacks are different from sensor failures. The attack signal is located in the range of normal sensed values so fault diagnosis and fault-tolerant control cannot detect the attack.

In order to protect the process control systems from critical sensor measurements compromised attacks, a threat assessment methodology is developed and attacks detection and response mechanisms are designed by Lin et al. [11]. Lin et al. proposes a model-based anomaly detection module (mADM) to protect the process control systems from compromised sensor attacks. By using mADM with the trained parameters, PCSs can avoid being attacked by DoS or integrity attacks. mADM sees sensor failures as attacks. When a sensor fails, mADM replaces the sensed signal with the simulated signal and send an alert to administrator.

In this thesis, we consider a more elaborated attack, stealthy attack, other than DoS or integrity attacks. Following the study of [11] experimenting and simulating on a realistic chemical reactor plant [12], [13], we play as an insider conducting a series of stealthy attacks. We evaluate the robustness of the defense mechanism by two cases, (1) an insider knows all the parameters of the mADM or (2) an insider obtains the permission to adjust the parameter settings.

1.2 Contributions

In this thesis, we design a general stealthy attack signal and propose three kinds of different stealthy attack models. By launching these stealthy attacks, we intend to analyze the pressure variation of the reactor to see the effectiveness of mADM protecting the system. Moreover, a way to evaluate the cost of the system is proposed to understand the changing before and after launching stealthy attacks. We analyze the abilities of stealthy attacks causing explosion to the reactor and increasing the cost of the system to evaluate the robustness of mADM.

1.3 Synopsis

This thesis is organized as follow. In Chapter 2, a general PCS, the TE-PCS, and the mADM are introduced in detail. Chapter 3 describes the stealthy attack models. Chapter 4 shows the experiments results after launching different kinds of stealthy attacks. In Chapter 5, effect of using different parameters of the mADM are analyzed. In addition, we evaluate the effect of stealthy attacks by seeing PPI variations indicating the system cost and by counting the earnings of products with different profits. Finally Chapter 6 concludes.

Chapter 2

Background

In this section, we will describe process control systems (PCSs), a well-studied process control system, Tennessee-Eastman process control system (TE-PCS) model [12], Ricker's proportional-integral (PI) control loops for the simplified TE process [13] and the mADM which is proposed by Lin et al. [11].

2.1 Process Control System (PCS)

PCSs are widely used in our daily life to monitor and control processes such as transmission, distribution of utility services, and manufacturing factories. Take modern water distribution for example. Waterworks receive monitored data of the tank levels, the pressure of storage tanks, pH, turbidity, and chlorine residual in the tanks from remote sensors. Depending on these data, waterworks control the pumps [14] or the gates [15] and addition of chemicals to the water [16], [17], [18]. The factory or the plant here, works under the instruction of control commands $u(k)$ at time k. And there are sensors monitoring the plant's statuses. Getting the sensed values $y(k)$ at time k from the sensors, the controllers give the control commands $u(k+1)$ for the next time slot $k+1$ depending on the control laws. The whole process can be shown as Fig. 2.1.

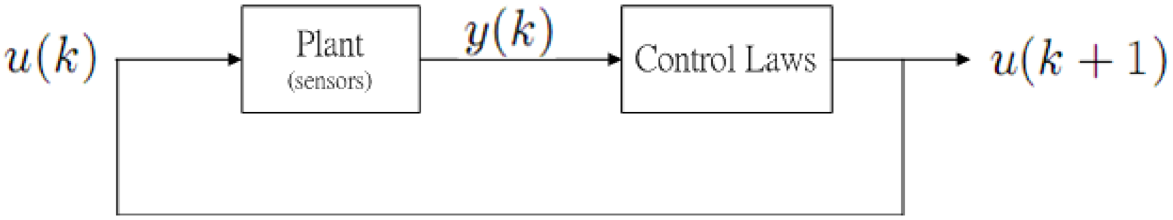

Figure 2.1: PCS

2.2 TE-PCS

In this subsection, we are going to introduce the TE-PCS that we use as our experimental environment in detail. The original complex TE-PCS model [12] is simplified by Ricker [13]. Originally there are 41 measured output variables and 12 manipulated variables but are reduced to 10 and 4. Ricker also proposes the multi-loop PI control laws to control the simplified TE process at the steady state. The chemical process comprises two non-condensable reactants A and C, an inert B, and non-volatile liquid product D.

$$A + C \xrightarrow{B} D$$

Three of the ten measured output variables (denoted by $y_i, i = 1, 2, 3$) are sensed by three sensors and are used in the multi-loop PI control laws to control the four manipulated variables. The objectives of the control laws are to regulate the production rate of product D at set-point F_4^{sp} ($kmol\ h^{-1}$), to keep pressure of the reactor P under the crash limit, $3000kPa$, and to maintain the ratio of ingredient A in reactor at set-point y_3^{sp} ($kmol\ h^{-1}$). Base on the objectives, Fig. 2.2 shows how Ricker's control loops work.

- Control loop 1:

  Control loop 1 includes product sensor S_1, loop 1 controller C_1, and feed 1 valve V_1. The production rate $F_4 = y_1$ is sensed by S_1 and is sent to C_1. After computing the control signal u_1, C_1 adjusts V_1 opening rate according to u_1. C_1 controls the amount of input ingredients F_1 bases on F_4^{sp} to regulate F_4.

- Control loop 2:

  Control loop 2 contains pressure sensor S_2, loop 2 controller C_2, and purge valve V_2. The pressure of the reactor $P = y_2$ is sensed by S_2 and is sent to C_2. After computing the control signal u_2, C_2 tunes V_2 opening rate according to u_2. C_2 controls P by letting less vapor in reactor out when P is over low comparing to P^{sp}, and vice versa.

- Control loop 3:

  Control loop 3 involves reactor sensor S_3, loop 3 controller C_3, and feed 2 valve V_3. The fraction of ingredient A in reactor y_3 is sensed by S_3 and is sent to C_3. After computing the control signal u_3, C_3 adjusts V_3 opening rate according to u_3. C_3 maintains y_3 at y_3^{sp} by adjusting V_3.

- Control loop 4:

  Control loop 4 is composed of pressure sensor S_2, loop 4 controller C_4, C_1 and V_1. When P was over high ($P^{max} = 2900kPa$), u_2 has the chance to saturate. Therefore C_4 changes set-point F_4^{sp} to shrink u_1 and further lower P.

These control loops helps the system to operate at the steady-state where the production rate $F_4 = y_1$ is $100kmol$, the pressure P is $2700kPa$, and the fraction of ingredient A in reactor y_3 is 47%.

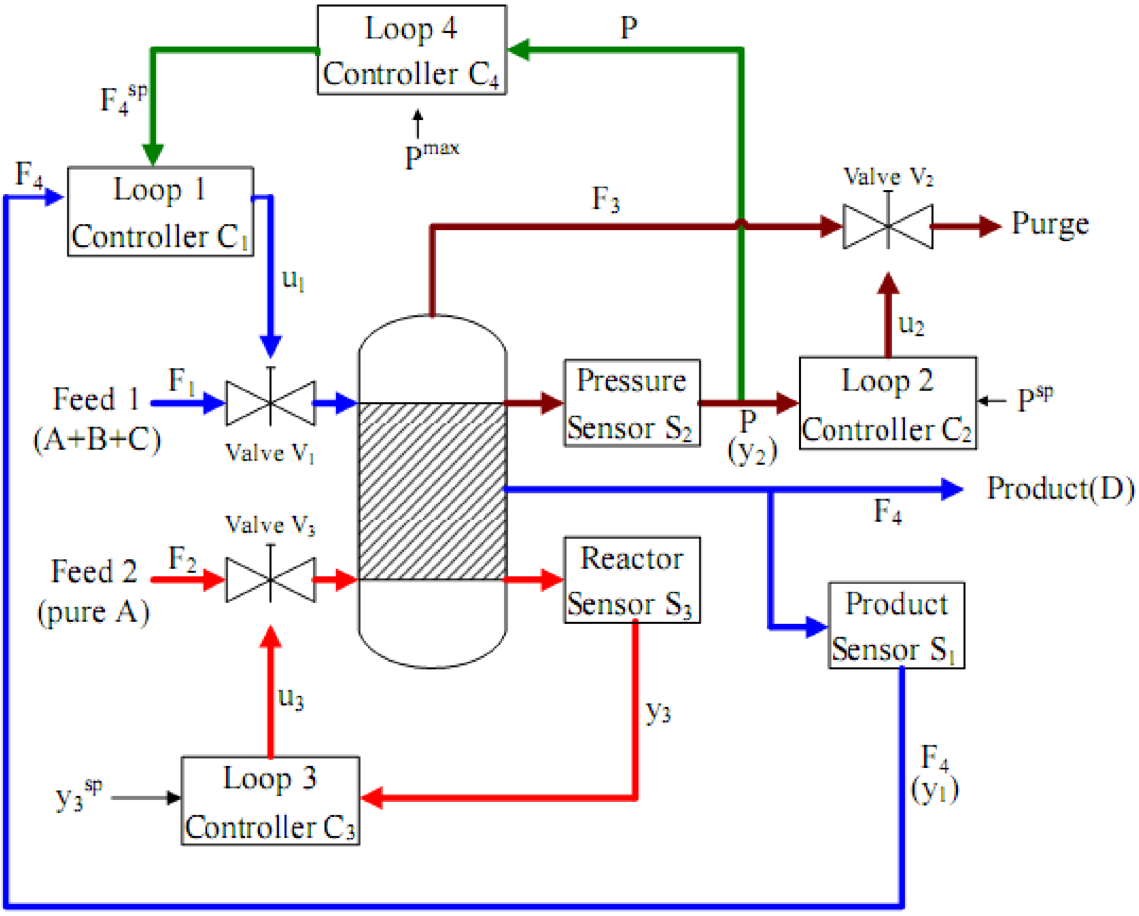

Figure 2.2: Simplified TE-PCS with four control loops

2.3 mADM

In [11], Lin et al. assess the new vulnerabilities and threats to PCSs (Fig. 2.3). He aims

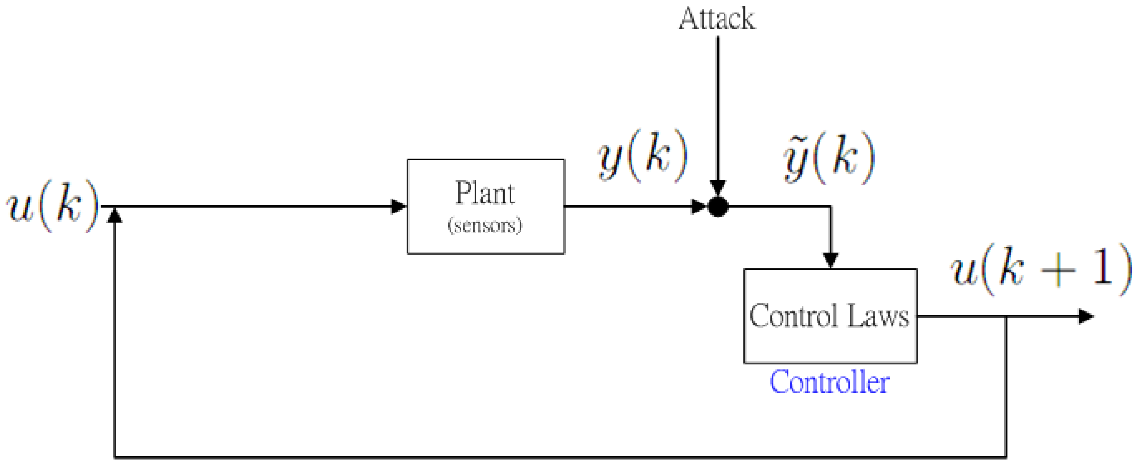

Figure 2.3: Threats to PCSs

at these aspects to attack the sensors' measurements. Then Lin et al. also proposes a mADM (Fig. 2.4) to defend these kinds of attacks.

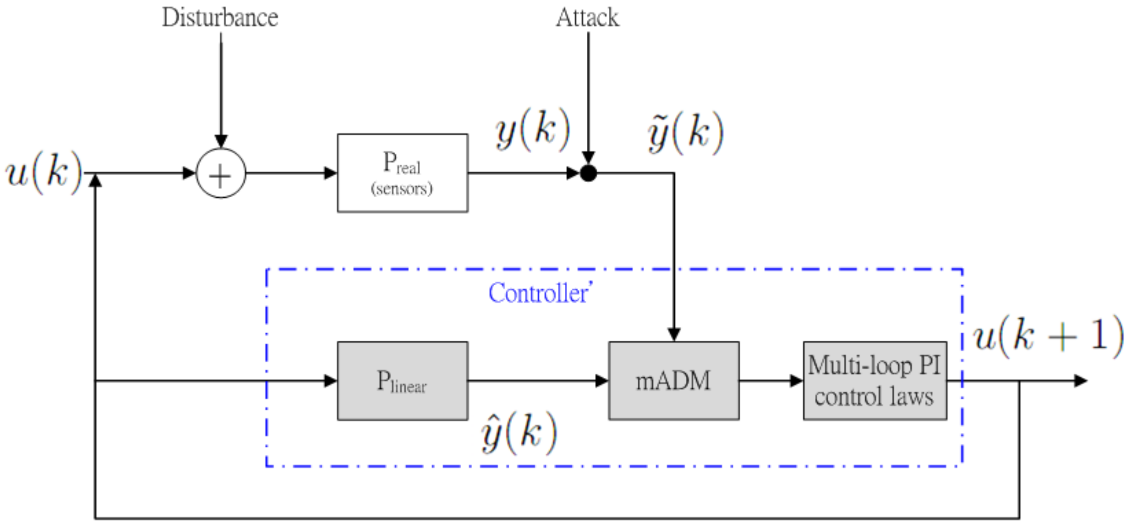

Figure 2.4: mADM

Lin et al. take simplified TE-PCS [13] to do his simulation. The main attacking goal that Lin et al. want to achieve is to drive the pressure of the TE reactor over 3000kPa (unsafe state).

It can be realized by launching attacks proposed in [19], [20], [21]. Lin et al. also add a Gaussian disturbance with variance 0.2 and zero mean to the control inputs $u(k)$ to make the system real-like. For defending these attacks, a mADM is proposed. In order to detect attacks, the module uses the cumulative sum mechanism to cumulate the output differences between the TE-PCS model ($\tilde{y}(k)$) and the representative model ($\hat{y}(k)$) at time k. The representative model is an internal linear model which satisfies the timing correctness in real time requirements. In each time slot k, the cumulative sum $S(k)$ equals to the differences between $\tilde{y}(k)$ and $\hat{y}(k)$ subtracted by a tolerated difference b and adds to the previous cumulative sum $S(k-1)$ (Eq. (2.1)).

$$S(k) = S(k-1) + |\tilde{y}(k) - \hat{y}(k)| - b, S(0) = 0 \tag{2.1}$$

$S(k)$ equals to zero when $S(k)$ is smaller than zero. Generally, $S(k)$ fluctuates around zero because the mean of the added disturbance is zero Fig. 2.5. When $S(k)$ is under the threshold τ, the controller uses the outputs of the simplified TE-PCS model. Once the cumulative sum exceeds τ, the mADM gives the outputs of the linear model to the controllers and sends out an alert to the administrator.

As shown in Fig. 2.6, b is the mean of the outputs difference between the simplified TE-PCS model under no attacks (the blue line) and the internal linear model (the green dotted line). τ is chosen by the tradeoff of false alarm rate and detection time. A mis-chosen b or τ affects the mADM seriously. If b is larger than it is supposed to be, the cumulative sum will never grow high enough to reach τ. In other words, the module will never have the chance to detect the attacks. On the contrary, if b is chosen smaller, the cumulative sum will cumulate because of the noise even when there is no attack. There will be false alarms all the time. A mis-chosen τ has the same bad effect to the system. Larger τ prolongs the detection time, and hence the module loses the prime time to discover an attack. The smaller τ may reduce the detection time. It is also easy to make the cumulative sum exceed τ and causes a false alarm. b and τ should

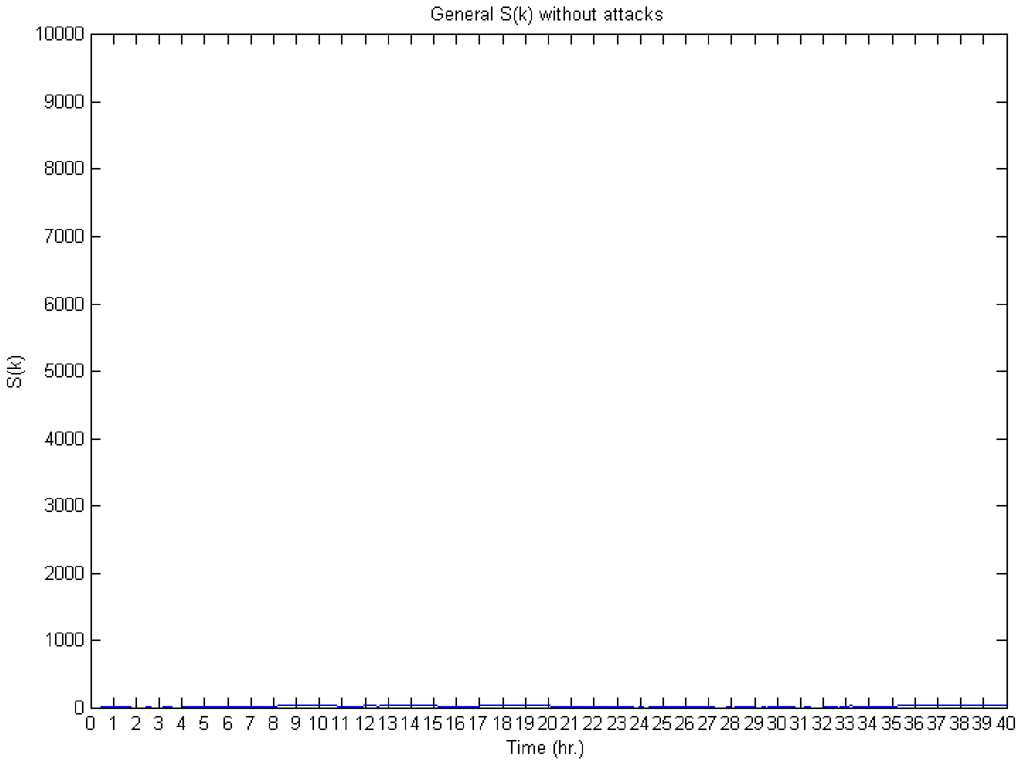

Figure 2.5: General S(k) without attacks

be carefully chosen before the module goes online, because these two parameters are the key points to make a robust mADM. Lin et al. set $b_{Lin} = [0.0629, 1.7868, 0.0151]$ and $\tau_{Lin} = [50$ 10000 200].

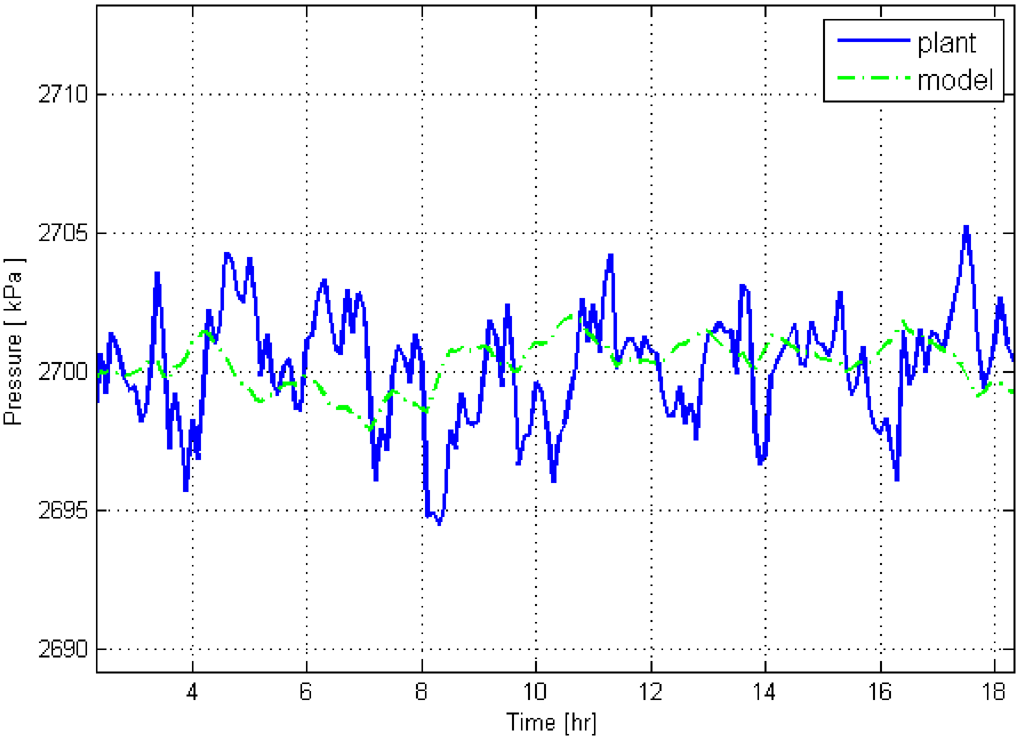

Figure 2.6: Difference between plant and linear internal model

Chapter 3

Modeling Stealthy Attacks

We now consider an insider (1) who knows every parameter including: the output of internal linear model $\hat{y}(k)$, b, and τ of the mADM or (2) the insider get the permission to modify b and τ. The insider may carry stealthy attacks that can avoid being detected by the mADM. Fake sensed values locating between the minimum and the maximum value sensed by a normal sensor are given to the mADM by the insider as stealthy attack signals. From Eq. (2.1), we know the detection scheme cumulates the difference between modified sensed value $\tilde{y}(k)$ and the output of internal linear model $\hat{y}(k)$. For the convenience to manipulate $S(k)$ under τ, we assume the insider designs the attack signals as $\tilde{y}(k) = \hat{y}(k) - \delta$. By nullifying $\hat{y}(k)$, the insider can manipulate δ as any values to make sure that $S(k)$ never exceeds τ.

We expand the causal equation $S(k) = S(k-1) + |\tilde{y}(k) - \hat{y}(k)| - b$ at time $k = n$ to have a clearer sight in making sure that $S(k)$ is always less than τ.

Theorem 1. *The increment quantity of $S(k)$ in period n is the summation of the output differences in period n between modified sensed value $\tilde{y}(k)$ and the internal linear model $\hat{y}(k)$ from $k = 1$ to $k = n$, and minuses nb.*

$$S(n) = \sum_{k=1}^{n} |\tilde{y}(k) - \hat{y}(k)| - nb \tag{3.1}$$

Proof. We shall prove the theorem by induction on n.

assume $S(0) = 0$

$$\textbf{let } k = 0 \Rightarrow S(0) = 0$$

$$k = 1 \Rightarrow S(1) = 0 + |\tilde{y}(1) - \hat{y}(1)| - b$$

$$\vdots$$

$$\textbf{if } k = n-1 \Rightarrow S(n-1) = \sum_{k=1}^{n-1} |\tilde{y}(k) - \hat{y}(k)| - (n-1)b \textbf{ holds}$$

by induction

$$k = n \Rightarrow S(n) = S(n-1) + |\tilde{y}(n) - \hat{y}(n)| - b = \sum_{k=1}^{n} |\tilde{y}(k) - \hat{y}(k)| - nb \textbf{ holds}$$

□

Let $n = k_x$, from Theorem 1, attacker can drive $S(k)$ from 0 to $S(k_x)$ in n slots. If attacker wants to drive $S(k)$ from $S(k_x)$ to $S(k_y)$ in next $n_1 = k_y - k_x$ slots, he can just simply add $\sum_{k=k_x+1}^{k_y} |\tilde{y}(k) - \hat{y}(k)| - n_1 b$ to $S(k_x)$. As in (Fig. 3.1), any attacks increase $S(k)$. This incremental curve is composed by convex curves, slopes, and concave curves if the curve is divided into several line segments. These three kinds of curves represent three kinds of attacking behaviors. Steeper slope of the curve implies stronger attack. Convex curve means the attack mitigates the strength when time passes by. Slope means the attack keeps same strength. As for the concave curve, the attack strength is enhanced with time. We model these three kinds of attacks as $\delta = \beta\alpha^{n-k}$, where β is a positive number varies with α and n. α is a positive constant determines the bending degree. $n = k_x - k_y$ is the attack duration and k is the time slot where $k_x < k \le k_y$ (Fig. 3.1).

By changing from $\alpha < 1$ to $\alpha > 1$ and with different n, we can model any arbitrary $S(k)$

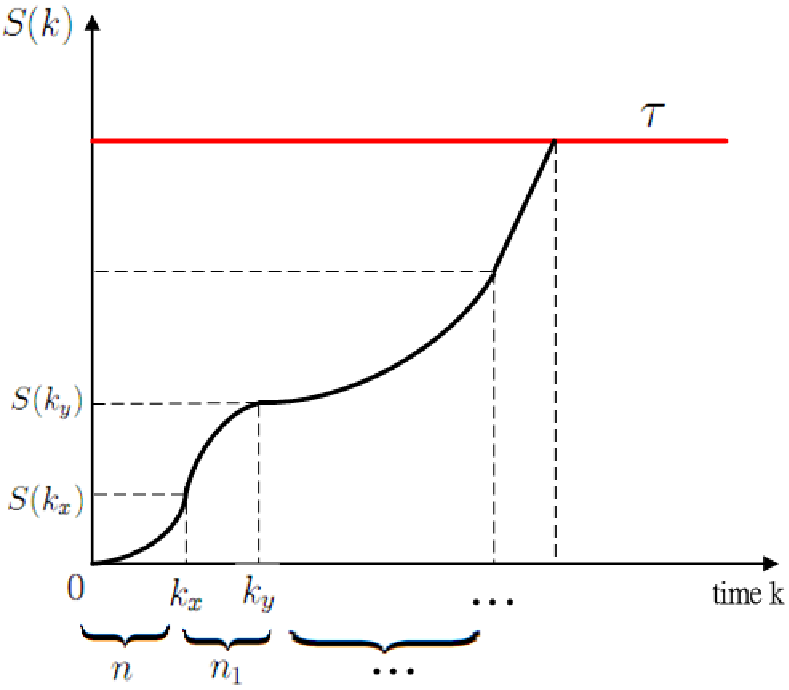

Figure 3.1: $S(k)$ curve under stealthy attack

curves. Hence a general formula for the stealthy attack signal is shown below:

$$\tilde{y}(k) = \hat{y}(k) - \beta\alpha^{n-k} \tag{3.2}$$

For simplicity, we assume the attack starts from $k_x = 0$ and ends at $k_y = n$. The cumulative sum reaches the threshold τ at time $k = n$ while the attack is ceased. Substituting $\tilde{y}(k)$ in Eq. (3.1) by Eq. (3.2), we can get Eq. (3.3). By choosing a constant α, the inside attacker can find an appropriate β that satisfies $S(n) \leq \tau$. The attacker can generate the stealthy attack signal by solving the equation

$$S(n) = \sum_{k=1}^{n} \beta\alpha^{n-k} - nb \leq \tau \tag{3.3}$$

Since α and n are chosen constants, from the formula of the first n term of geometric series with the common ratio $\neq 1$, $\beta = \frac{\tau+nb}{\frac{1-\alpha^n}{1-\alpha}}$ can be solved.

According to the constant value of α, we categorize stealthy attacks into three types: *convex curve (cv), slope (sl), and concave curve (cc) attacks*.

3.1 Convex Curve (cv) Attacks

In a convex curve attack, the attacker makes the maximum damage to the system in a short time period. By Eq. (3.2), this kind of attack signal can be generated by choosing $\alpha > 1$. In Fig. 3.2, $S(k)$ approaches τ very fast at the beginning of the attack but slow down when k is close to n and stop growing at $k = n$. Since slope $x_1 > x_2$, we know the strength of the attack is strong at the beginning but diminishes at the rest of the attack duration. The strong variance at the beginning may cause high attention. Hence cv attack may not be so harmful.

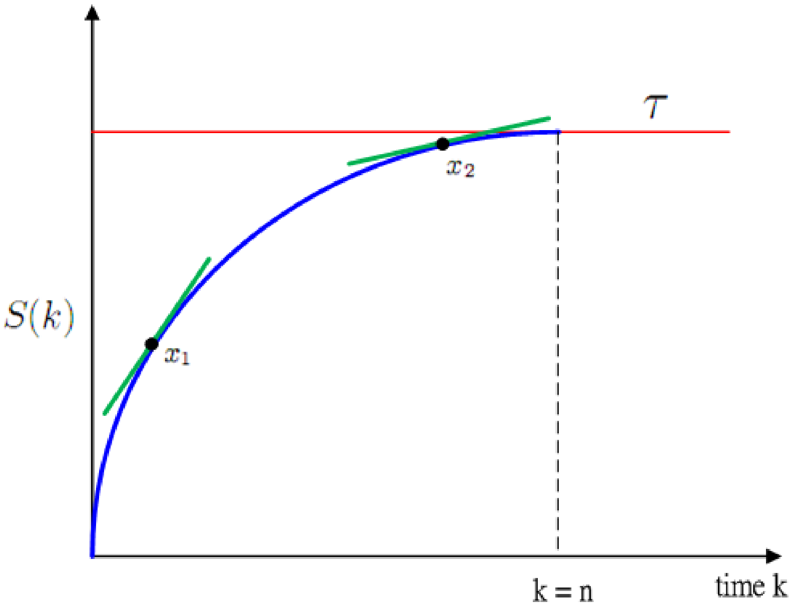

Figure 3.2: $S(k)$ of a cv attack

3.2 Slope (sl) Attacks

In a slope attack, the attacker keeps attack signal $\tilde{y}(k)$ a constant difference δ to $\hat{y}(k)$ which means selecting $\alpha = 1$ in Eq. (3.2). So the equation

$$\sum_{k=0}^{n-1} \beta\alpha^{n-k} - nb = \tau$$

is reduced to $n\beta - nb = \tau$. When $\beta = b + \tau/n$, $S(k)$ is a constant slope (Fig. 3.3) growing from attack starts and reaching τ at the end of the attack ($k = n$). There is no variance strength in this kind of attacks because the slope is always the same. sl attack always keeping the same pace is a moderate attack comparing to cv and cc attacks.

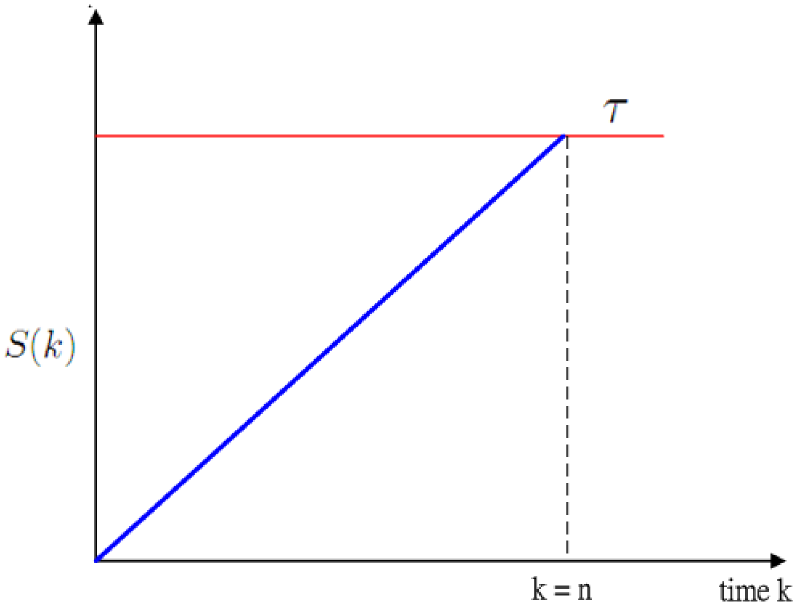

Figure 3.3: $S(k)$ of a sl attack

3.3 Concave Curve (cc) Attacks

In a concave curve attack, the attacker chooses $\alpha < 1$ in Eq. (3.2), which causes serious damage at the end of the attack instead of the beginning. $S(k)$ is a contrast to cv. We can see in Fig. 3.4, $S(k)$ starts slowly and ends severely to reach τ at time $k = n$. The slope of cc is always larger ($x_1 < x_2$) one time slot after another so we know that the strength keeps stronger all the time. Hence cc may cause severer damage than cv and sl attacks.

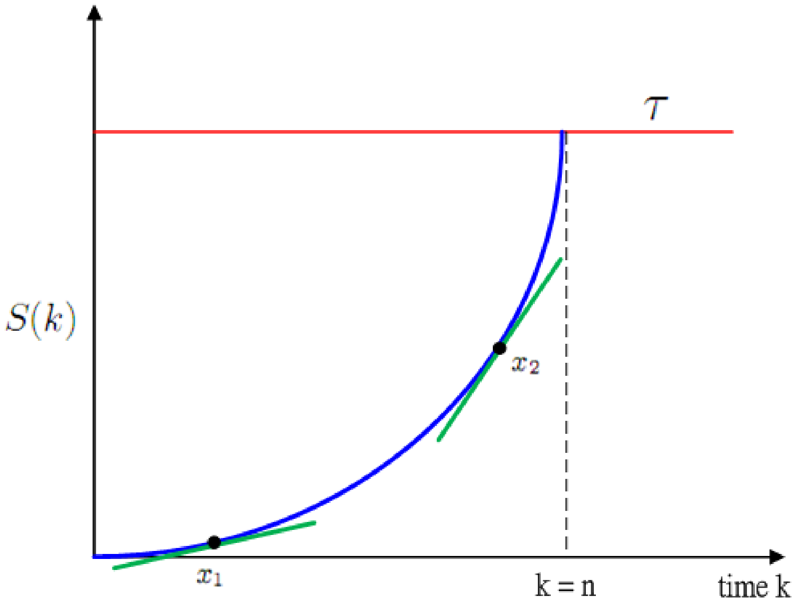

Figure 3.4: $S(k)$ of a cc attack

Chapter 4

Experiments

In this chapter, we run the three kinds of stealthy attacks mentioned above to test how much damage these attacks can cause to the explosion of the reactor. The experiments settings are as following:

4.1 Setup

In order to see how the stealthy attacks will affect the TE-PCS with the mADM proposed by Lin et al. , we use the following three components to simulate the experiments:

- TE-PCS model: The model written in .f file should be compiled into .mexw32 format by Intel Visual FORTRAN compiler ver. 11. 0. The codes can be got by sending an e-mail to ricker@cheme.washington.edu

- PI control laws: The codes written in .M file running on MATLAB ver. 7. 8. 0. 347 can be got by sending an e-mail to ricker@cheme.washington.edu

- mADM: The codes written in .M files running on MATLAB ver. 7. 8. 0. 347 can be got by sending an e-mail to rekociv@gmail.com

4.2 Experiments

We design a formal format for stealthy attack which can be represented by 5 tuple as $\{< A, S, T_s, T_e, \tau_{sa} >^+\}$.

- A: the type of stealthy attack (cv, sl, or cc)
- S: the victim sensor (S_1, S_2, or S_3)
- T_s: the time that attack starts
- T_e: the time that attack ends
- τ_{sa}: the value that $S_i(k)$ reaches

In addition, $^+$ indicates one or more sensors are attacked. In this section, we design experiments launching cv, sl, and cc attacks mentioned in the previous chapter. For an insider knowing the parameters of mADM, we conduct Exp#1 and Exp#2 to find the weakest sensor and the relative type of stealthy attack. In Exp#3 we launch the most effective attacks derived from the first two experiments on sensors with different starting time to find the most effective attack timing. For an insider getting the authority to configure the parameters of mADM, we conduct Exp#4 and Exp#5 to see the robustness of mADM with different bs and τs.

4.2.1 Exp#1: Effect of Different Attacks

In the first experiment (Exp#1), we want to know what type of attack is more effective in driving the pressure up for each sensor. Thus we launching different attacks on different sensors in Exp#1. 1$\sim$Exp#1. 9 (Table 4.1).

In Exp#1, b and τ are the best values recommended by Lin et al. , $b = b_{Lin} = [0.0629, 1.7868, 0.0151]$ and $\tau = \tau_{Lin} = [50\ 10000\ 200]$. The experiment can be represented as $\{< cc,$

Table 4.1: Exp#1: Effect of Different Attacks

Exp#	S	T_s	T_e	τ	Results
1.1	S_1/cc	0	1~40	50	Fig. 4.1
1.2	S_1/sl				
1.3	S_1/cv				
1.4	S_2/cc			10000	Fig. 4.2
1.5	S_2/sl				
1.6	S_2/cv				
1.7	S_3/cc			200	Fig. 4.3
1.8	S_3/sl				
1.9	S_3/cv				

S_1, 0, 1~40, 50>}, {< sl, S_1, 0, 1~40, 50>}, {< cv, S_1, 0, 1~40, 50>}, {< cc, S_2, 0, 1~40, 10000>}, {< sl, S_2, 0, 1~40, 10000>}, {< cv, S_2, 0, 1~40, 10000>}, {<cc, S_3, 0, 1~40, 200>}, {< sl, S_3, 0, 1~40, 200>}, and {< cv, S_3, 0, 1~40, 200>}. For Exp#1. 1~Exp#1. 3 we start the attacks from $T_s = 0$ and end the attacks at $T_e = 1$ to $T_e = 40$. Driving the $S(k)$ to 50, we stealthily attack S_1 by cv, sl, and cc attacks to see which types of attack is more effective in driving up the reactor's pressure. Similarly, we attack S_2 in Exp#1. 4~Exp#1. 6 and S_3 in Exp#1. 7~Exp#1. 9.

4.2.2 Exp#2: Effect of Attacking Two Sensors

In the second experiment (Exp#2), we consider the effect of attacking two sensors at a time when driving up the pressure of the reactor. Hence we design the attack as show in Table 4.2.

In Exp#2, b and τ are also the best values recommended by Lin et al. , $b = b_{Lin}$ and $\tau = \tau_{Lin}$. The experiment can be represented as {< cv, S_1, 0, 1~40, 50>, < cc, S_2, 0, 1~40, 10000>}, {< cv, S_1, 0, 1~40, 50>, < sl, S_2, 0, 1~40, 10000>}, {< cv, S_3, 0, 1~40, 200>, < cc, S_2, 0,

Table 4.2: Exp#2: Effect of Attacking Two Sensors

Exp#	S_I	S_{II}	T_s	T_e	τ_I	τ_{II}	Results
2.1	S_1/cv	S_2/cc	0	1∼40	50	10000	Fig. 4.4a
2.2		S_2/sl					Fig. 4.4b
2.3	S_3/cv	S_2/cc			200		Fig. 4.4c
2.4		S_2/sl					Fig. 4.4d

1∼40, 10000>}, and {< cv, S_3, 0, 1∼40, 200>, < sl, S_2, 0, 1∼40, 10000>}. Here we attack S_1 from $T_s = 0$ to $T_e = 1 \sim 40$ to drive the $S(k)$ to 50. At the meanwhile, we also attack S_2 from $T_s = 0$ to $T_e = 1 \sim 40$ to drive the $S(k)$ to 10000. Similarly, we attack S_2 and S_3 at a time. Comparing to the results in Exp#1, we can see the effect of attacking two sensors at a time.

4.2.3 Exp#3: Effect of Different Attack Timing

In the third experiment (Exp#3), we consider the effect of attacking two sensors with different starting time when driving up the pressure of the reactor. Hence we design the attack as show in Table 4.3.

Table 4.3: Exp#3: Effect of Different Attack Timing

Exp#	S_I	S_{II}	T_{s_I}	T_{e_I}	$T_{s_{II}}$	$T_{e_{II}}$	τ_I	τ_{II}	Highest Pressure
3.1	S_3/cv	S_2/cc	1∼20	4∼26	0	6∼12	200	10000	2922kPa
3.2			0	3∼6	1∼20	7∼32			2910.2kPa

In Exp#3, b and τ are also the best values recommended by Lin et al. , $b = b_{Lin}$ and $\tau = \tau_{Lin}$. The experiment can be represented as {< cv, S_3, 1∼20, 4∼26, 200>, < cc, S_2, 0, 6∼12, 10000>} and {< cv, S_3, 0, 3∼6, 200>, < cc, S_2, 1∼20, 7∼32, 10000>}. In Exp#3.1 we attack S_3 for 3~6 hours starting from $T_s = 1 \sim 20$ to drive the $S(k)$ to 200. We also attack S_2 from $T_s = 0$ to $T_e = 6 \sim 12$ to drive the $S(k)$ to 10000. In Exp#3.2 we attack S_3 for 3~6 hours starting from $T_s = 0$ to drive the $S(k)$ to 200. We also attack S_2 for $6 \sim 12$ hours starting from $T_s = 1 \sim 20$ to drive the $S(k)$ to 10000. Comparing to the results in Exp#2, we can see the effect of attacking two sensors at different timing.

4.2.4 Exp#4: Effect of Different b

From Eq. (3.3), we know that b and τ are the factors to determine the strength of a stealthy attack. In the fourth experiment (Exp#4), we like to know if an insider gets the authority to configure the b of the mADM, how dangerous the system will be. Here we fix $\tau = \tau_{Lin}$, and vary b from 0.5, 10, 20, to 40 times of b_{Lin} to driving the pressure of the reactor with S_2 and S_3 are attacked. The parameters of Exp#4. 1~ Exp#4. 4 are shown in Table 4.4.

Table 4.4: Exp#4: Effect of Different b

Exp#	S_I	S_{II}	T_s	T_e	τ_I	τ_{II}	times of b_{Lin}	Results
4.1	S_3/cv	S_2/cc	0	1~40	200	10000	0.5	Fig. 4.5a
4.2							10	Fig. 4.5b
4.3							20	Fig. 4.5c
4.4							40	Fig. 4.5d

In Exp#4 $\tau = \tau_{Lin}$ and b are 0.5/10/20/40 times of b_{Lin} (b =0.5$*b_{Lin}$, b =10$*b_{Lin}$, b =20$*b_{Lin}$, and b =40$*b_{Lin}$). The experiment can be represented as $\{<$ cv, S_3, 0, 1~40, 200$>$, $<$ cc, S_2, 0, 1~40, 10000$>\}$. Here we attack S_2 by cc from $T_s = 0$ to $T_e = 1 \sim 40$ to drive the $S(k)$ to 10000. At the meanwhile, we also attack S_3 by cv from $T_s = 0$ to $T_e = 1 \sim 40$ to drive the $S(k)$ to 200. With different multiples of b_{Lin}, we can see the effect of b protecting the system.

4.2.5 Exp#5: Effect of Different τ

In the fifth experiment (Exp#5), we like to know if the insider configures different τ for the mADM how will that effect the pressure of the reactor when S_2 and S_3 are attacked. From Eq. (3.3), we can see that τ is the dominant factor to decide the strength of a stealthy attack. To adjust the value of τ to 1.5/0.5 of τ_{Lin}, it is enough to see the effect. Hence we design the attacks as in Table 4.5.

Table 4.5: Exp#5: Effect of Different τ

Exp#	S_I	S_{II}	T_s	T_e	τ_I	τ_{II}	Results
5.1	S_3/cv	S_2/cc	0	1∼40	100	5000	Fig. 4.6
5.2					300	15000	Fig. 4.7

In Exp#5 $b = b_{Lin}$ and τ are 1.5/0.5 times of τ_{Lin} ($\tau =$ [75 15000 300] and $\tau =$ [25 5000 100]). The experiment can be represented as {$<$ cv, S_3, 0, 1∼40, 300$>$, $<$ cc, S_2, 0, 1∼40, 15000$>$}, {$<$ cv, S_3, 0, 1∼40, 100$>$, $<$ cc, S_2, 0, 1∼40, 5000$>$}. Here we attack S_2 by cc from $T_s = 0$ to $T_e = 1 \sim 40$. At the meanwhile, we also attack S_3 by cv from $T_s = 0$ to $T_e = 1 \sim 40$. Driving the $S(k)$s to different values, we can see the effect of τ protecting the system.

4.3 Experiments Results

The following subsections show the results of Exp#1, Exp#2, Exp#3, Exp#4, and Exp#5. We will see how the pressure of the reactor varies with the five different experimental designs.

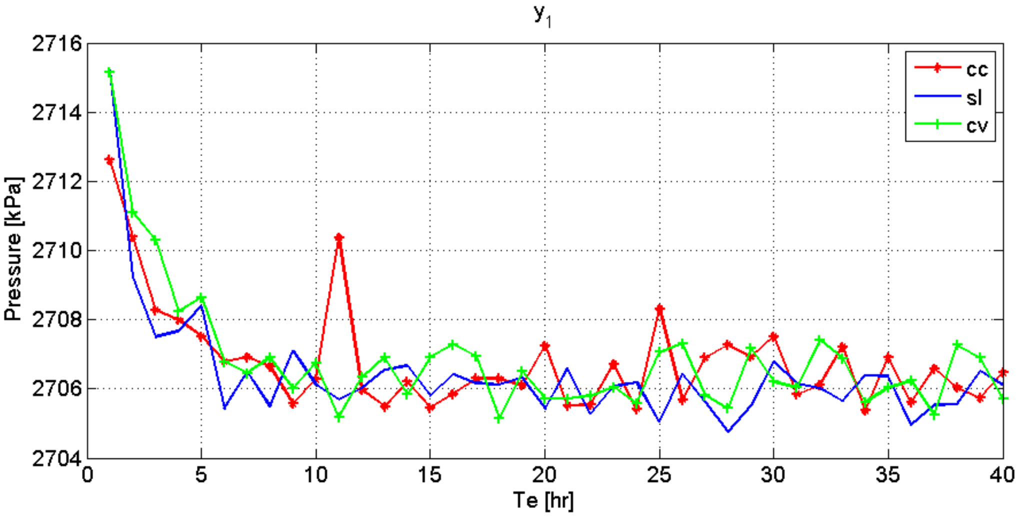

Figure 4.1: Pressure of the reactor under 3 types of stealthy attacks on S_1 starts from 0 hr and ends at 1$\sim$ 40 hrs

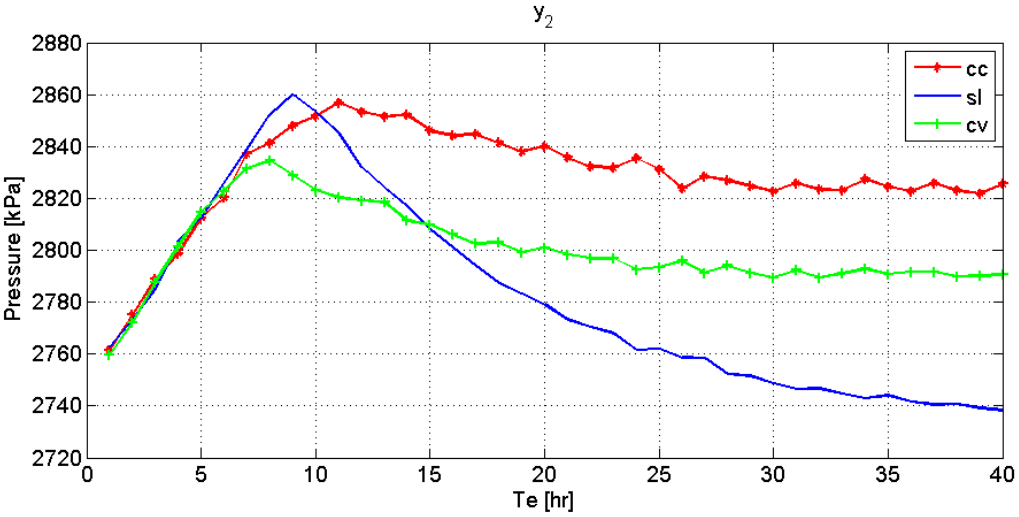

Figure 4.2: Pressure of the reactor under 3 types of stealthy attacks on S_2 starts from 0 hr and ends at 1$\sim$ 40 hrs

4.3.1 Exp#1: Effect of Different Attacks

From Fig. 4.1, we know that no matter what kinds of attack we applied to S_1, they are equally not useful to drive up the pressure. When attacks end at 1$\sim$40 hrs, the pressure is driven up a little bit higher but it is still very close to steady state pressure (2700kPa). From Fig. 4.2, we see that attacking S_2 can efficiently drive the pressure high, especially sl for short attack duration and cc for long attack duration. For S_3, the pressure is driven up under short attack duration. Long attack duration has poor effect in driving up the pressure (Fig. 4.3).

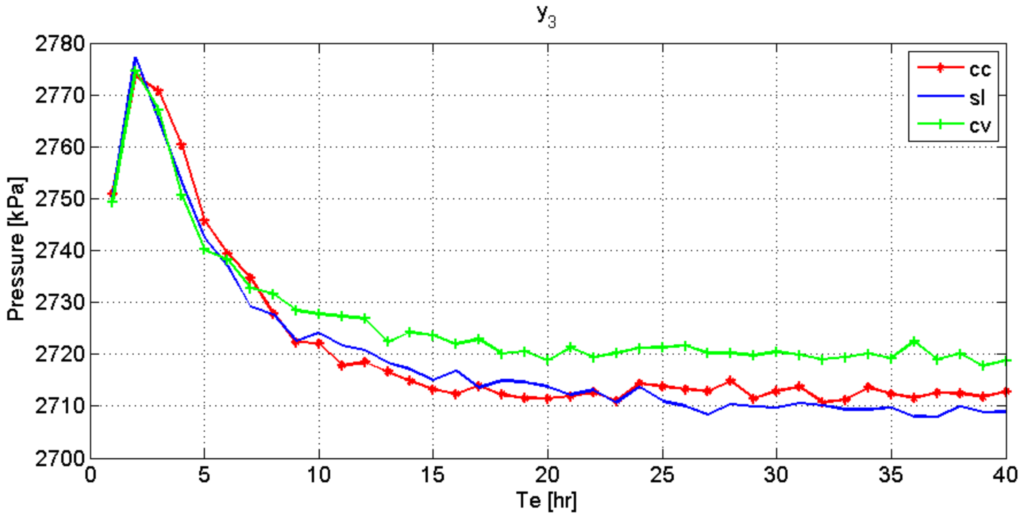

Figure 4.3: Pressure of the reactor under 3 types of stealthy attacks on S_3 starts from 0 hr and ends at 1∼ 40 hrs

In Fig. 4.1, Fig. 4.2, and Fig. 4.3, when attack duration is less than 6 hrs, the three types of attacks have almost the same effect in driving up the pressure for three sensors. It is reasonable because when attack duration is small, three types of attacks behave like sl. From Fig. 4.1, Fig. 4.2, and Fig. 4.3, attacking S_2 to drive the pressure up is efficient. Thus we say that S_2 is the key sensor to be attacked in stealthy attack for driving up the pressure. The reason is that S_2 is the basis in controlling the opening degree of purge valve which is the main component to regulate the pressure. Thus we launch different combination of attacks with S_2 for the following experiments. In Fig. 4.1, the pressure that cv can drive up to looks a bit higher than cc and sl and it is also true in Fig. 4.3. As for Fig. 4.2, we can hardly tell sl is better than cc or not. In the following experiments, for S_1 and S_3, we attack them by cv and for S_2, we do both cc and sl.

4.3.2 Exp#2: Effect of Attacking Two Sensors

In Exp#2, when we attack S_1 and S_2 together (Fig. 4.4a and Fig. 4.4b), the highest pressure we can reach is not far away from only attacking S_2. It matches the result in Exp#1 which is, attacking S_1 cannot drive up the pressure efficiently. We also see that line segments $\overline{B}$ in Fig. 4.4a and Fig. 4.4b are straight. It implies there is no special attack duration while launching attacks on S_1.

On the other hand, attacking S_2 and S_3 together can improve the result a lot (Fig. 4.4c, and Fig. 4.4d). Point A in Fig. 4.4c indicates the highest pressure (2937.6kPa) happens at attacking S_2 by cc for 5 hrs and attacking S_3 by cv for 6 hrs. From point A in Fig. 4.4c and Fig. 4.4d, we know that the best attack duration on S_3 is about 3∼6 hrs. From the four subfigures in Fig. 4.4, the crest lines ($\overline{B}$) tells that the best attack duration for S_2 is about 6∼12 hrs.

4.3.3 Exp#3: Effect of Different Attack Timing

In Exp#3, we attack S_2 for 6∼12 hours (the best attack duration derived from Exp#2) and attack S_3 for 3∼6 hours. The delayed attacking timing on S_3 is 1∼20 hours after launching cc on S_2. The highest pressure we can reach is 2922kPa. When we attack S_3 for 3∼6 hours and attack S_2 for 6∼12 hours with the delayed attacking timing on S_2 is 1∼20 hours after launching cv on S_3, we can get the highest pressure about 2910.2kPa. Both of the highest pressures are lower than the highest pressure (2937.6kPa) while attacking S_2 and S_3 at the same time. Thus we say the most effective attacking way is attacking S_2 and S_3 with the same T_s.

4.3.4 Exp#4: Effect of Different b

In Exp#4, we see that the highest pressure of 0.5 times of b_{Lin} (point A in Fig. 4.5a) is about the same with of b_{Lin} (point A in Fig. 4.4c). When b is 10, 20 or 40 times of b_{Lin}, the highest pressure grows higher and higher while b increases (point A in Fig. 4.5b $<$ point A in Fig. 4.5c $<$ point A in Fig. 4.5d). Notice that the system can be crashed (pressure over 3000kPa) if b is over 40 times of b_{Lin}. From Fig. 4.5d, pressures around point A are over 3000kPa. This is because the attack strength δ is affected by b. If b is larger, then the attacking strength becomes stronger and the pressure will be driven higher. The $S(k)$ will not reach τ faster while δ is stronger because in every time slot $S(k)$ is also subtracted by a larger b. Once b is over 40 times of b_{Lin}, the system is under the danger of exploding (point A valued 3017.8kPa is over 3000kPa in Fig. 4.5d).

4.3.5 Exp#5: Effect of Different τ

In Exp#5, when τ is 0.5 times of τ_{Lin}, we can clearly see that the highest pressure 2851.7kPa (point A in Fig. 4.6) is much lower comparing to the highest pressure 2937.6kPa of using τ_{Lin} (point A in Fig. 4.4c). This is because the attack strength δ is bounded by τ. If τ is half of τ_{Lin}, then the strength becomes minor and the pressure will not be driven so high. On the contrary, if τ is 1.5 times of τ_{Lin}, the pressure (point A valued 3005.8kPa in Fig. 4.7) is much higher than in Fig. 4.4c. We conclude that if τ is larger, then a stronger attack signal can be produced. With a larger τ, stealthy attack has better ability to drive the pressure higher and even to explode the reactor.

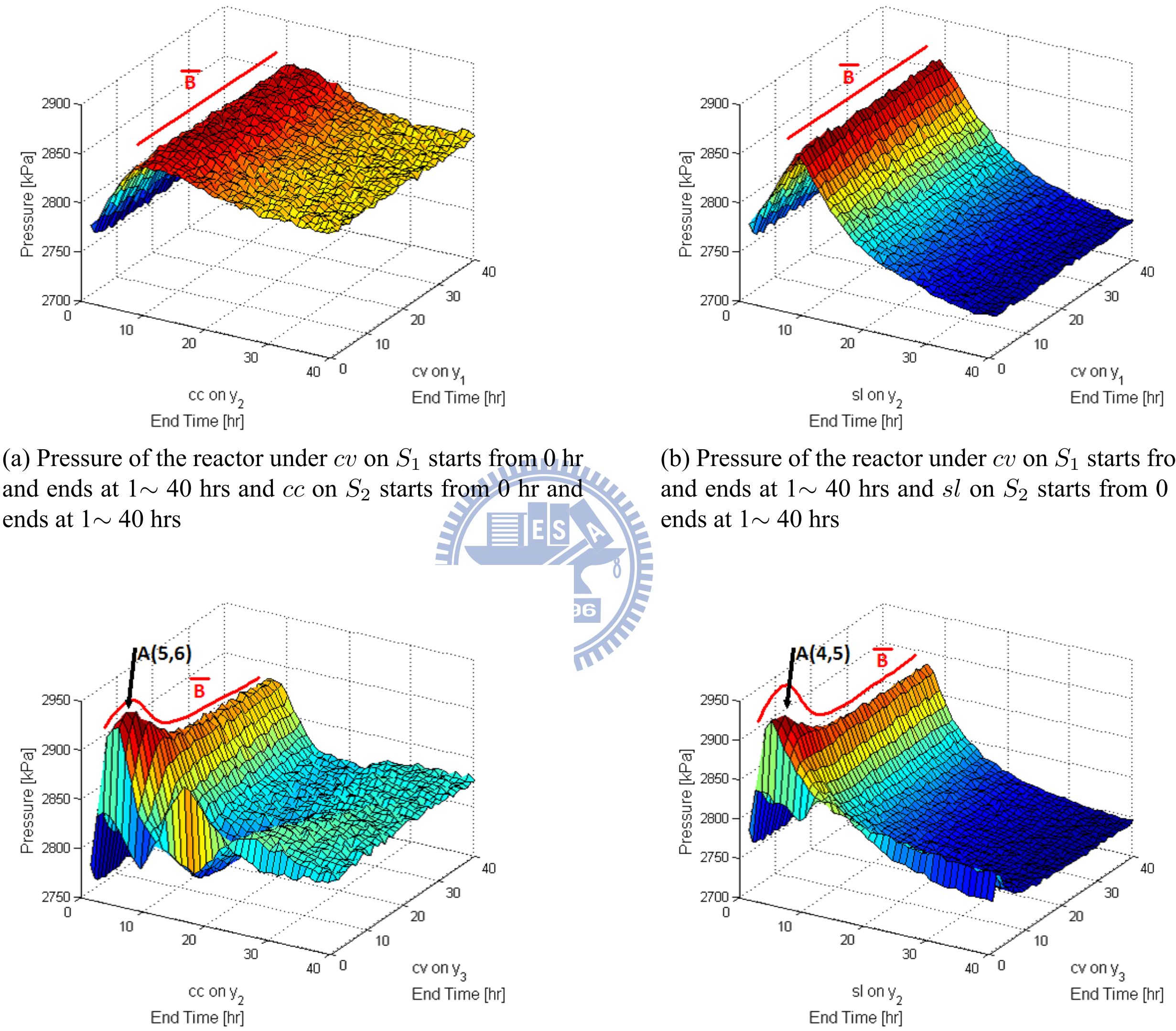

(a) Pressure of the reactor under cv on S_1 starts from 0 hr and ends at 1∼ 40 hrs and cc on S_2 starts from 0 hr and ends at 1∼ 40 hrs

(b) Pressure of the reactor under cv on S_1 starts from 0 hr and ends at 1∼ 40 hrs and sl on S_2 starts from 0 hr and ends at 1∼ 40 hrs

(c) Pressure of the reactor under cv on S_3 starts from 0 hr and ends at 1∼ 40 hrs and cc on S_2 starts from 0 hr and ends at 1∼ 40 hrs

(d) Pressure of the reactor under cv on S_3 starts from 0 hr and ends at 1∼ 40 hrs and cc on S_2 starts from 0 hr and ends at 1∼ 40 hrs

Figure 4.4: Pressure of two sensors attacked

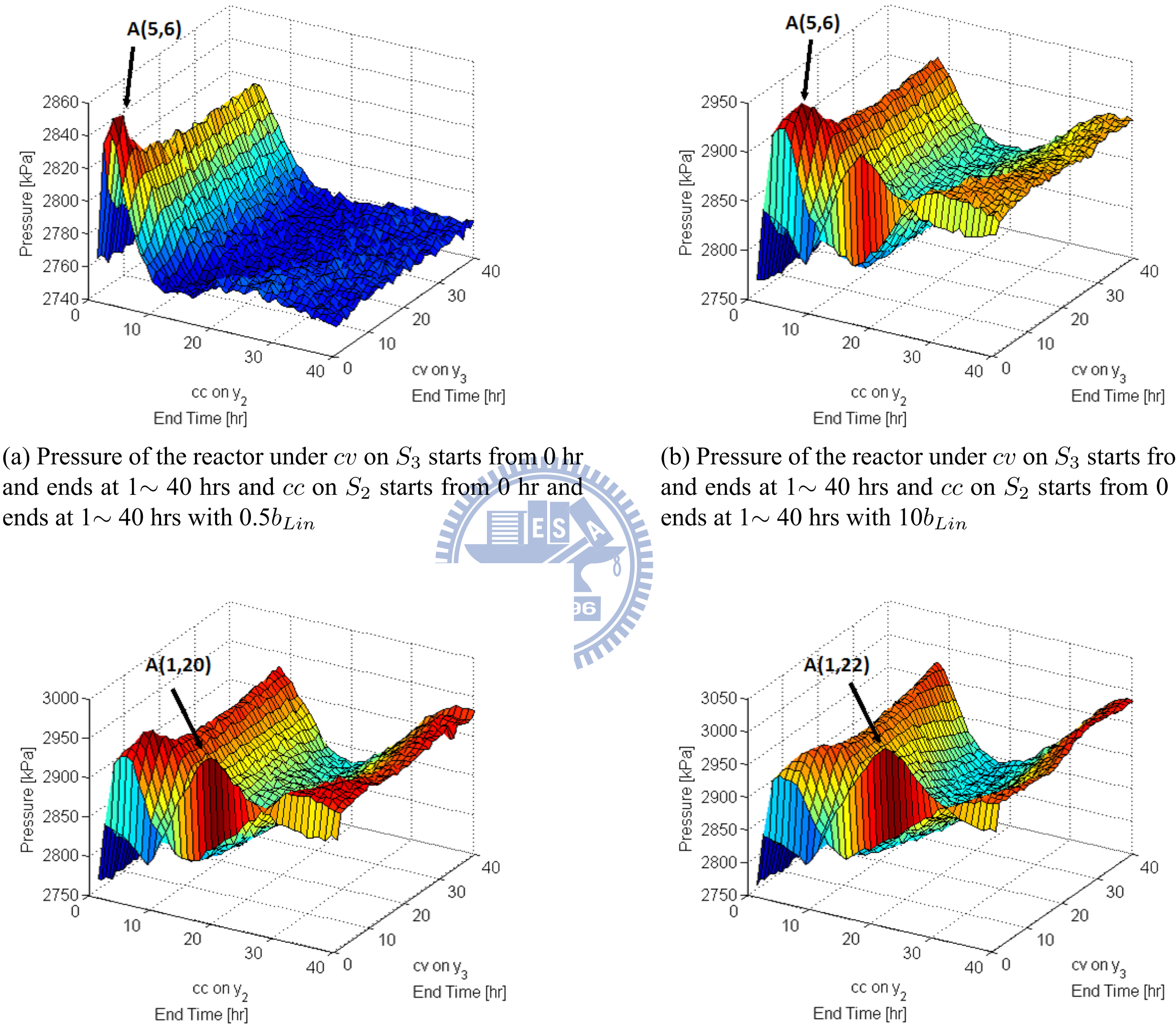

(a) Pressure of the reactor under cv on S_3 starts from 0 hr and ends at 1∼ 40 hrs and cc on S_2 starts from 0 hr and ends at 1∼ 40 hrs with $0.5b_{Lin}$

(b) Pressure of the reactor under cv on S_3 starts from 0 hr and ends at 1∼ 40 hrs and cc on S_2 starts from 0 hr and ends at 1∼ 40 hrs with $10b_{Lin}$

(c) Pressure of the reactor under cv on S_3 starts from 0 hr and ends at 1∼ 40 hrs and cc on S_2 starts from 0 hr and ends at 1∼ 40 hrs with $20b_{Lin}$

(d) Pressure of the reactor under cv on S_3 starts from 0 hr and ends at 1∼ 40 hrs and cc on S_2 starts from 0 hr and ends at 1∼ 40 hrs with $40b_{Lin}$

Figure 4.5: Pressure of two sensors attacked with different b

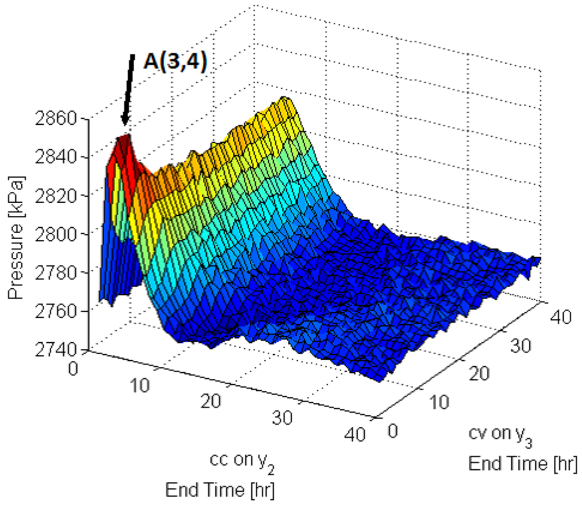

Figure 4.6: Pressure of the reactor under cv on S_3 starts from 0 hr and ends at 1∼ 40 hrs and cc on S_2 starts from 0 hr and ends at 1∼ 40 hrs with $0.5\tau_{Lin}$

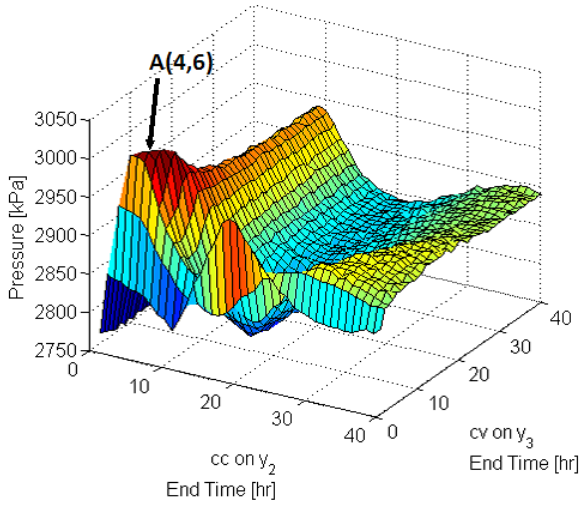

Figure 4.7: Pressure of the reactor under cv on S_3 starts from 0 hr and ends at 1∼ 40 hrs and cc on S_2 starts from 0 hr and ends at 1∼ 40 hrs with $1.5\tau_{Lin}$

Chapter 5

Analysis

There are two goals for an attacker to raise the cost while launching stealthy attacks on TE-PCS under the protection of the mADM. One is the attacker wishes to do his utmost to crash the system, which causes enormous cost to the entire environment when the reactor explodes. The other goal is to increase the cost and lower the profit of the system.

5.1 Environmental Cost

The completeness of the reactor is critically important to the whole environment. From Exp#1 and Exp#2, we know that the system may maintain the completeness under the protection of mADM with b_{Lin} and τ_{Lin}. From Exp#3 and Exp#4, once the insider get the authority to configure improper b and τ, the system is in crashing danger. If the over high pressure causes an explosion, it will be an un-estimated disaster. Losses of staffs', residents', and ecology's lives are beyond redemption. In the following subsection we will discuss the ranges to select proper b and τ for building a robust mADM.

5.1.1 Select a Proper b

In [11], we know b is determined by counting the average output difference between the system and the linear internal model in a pure environment which means without any attacks. The best b_{Lin} suggested by Lin et al. for sensor S_1, S_2, and S_3 are 0.0629, 1.7868, and 0.0151.

If the insider has the authority to configure a b other than b_{Lin}, from Exp#3, the system is under explosion danger while a larger b is used in mADM. The upper bound of choosing b should be less than $40b_{Lin}$. If b is smaller than b_{Lin}, it cannot eliminate the difference between real plant and internal linear model. $S(k)$ cumulates and false alarms occur. Therefore, we say a safe b for the system should be locate in b_{Lin} to $40b_{Lin}$.

5.1.2 Select a Proper τ

The τ is determined by the false alarm rate and detection time in [11]. Lin et al. sets τ_{Lin} for sensor S_1, S_2, and S_3 to 50, 10000, and 200. We scale the τ with different times to run the false alarm rate experiments and stealthy attacks to crash the system for 5000 runs. We get the plot below Fig. 5.1. Low τ (smaller than [15 3000 60]) causes false alarms and increases the management cost. Once the insider configures a high τ (over [55 11000 220]), there is a possibility of system crash. Therefore the attacker has the chance to achieve his goal to damage the environment.

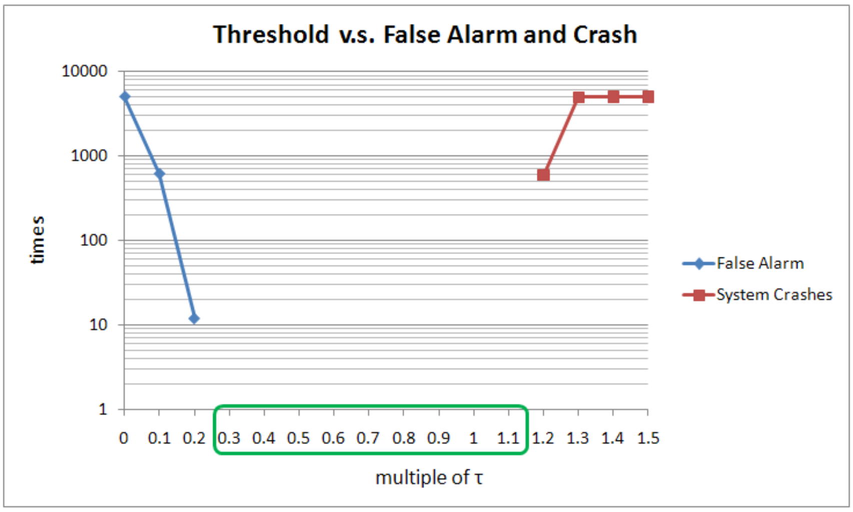

Figure 5.1: Range of choosing a good τ

There may be no way to crash the system under the mADM protection with proper b and τ located in the safe range. An insider gets the authority to configure improper b and τ is also a vital issue. In building a robust defensive mechanism for the mADM, choosing tolerated difference b and threshold τ is the key point. A bad choice increases the false alarms, or makes the system easily to be crashed by attackers.

5.2 Cost Evaluation

If the defender has chosen a proper τ and a reasonable b, the attacker will has to seek for what is less attractive than crashing the system. The attacker can achieve his goal by increasing the cost of the system. We consider the price-performance index of the system while under stealthy attacks. Price-performance index as known as PPI is an index to evaluate the efficiency of a system. Here are some aspects which should be considered when calculating PPI of TE-PCS: management cost (C_{mn}), operation cost (C_{op}), depreciation (C_{de}), material cost (C_{mt}), and sales revenue (R_{sl}).

$$C_{mn} = N_{al} \times W_{mn} \tag{5.1}$$

Management cost (C_{mn}) is the product of number of alarms (N_{al}) and cost of checking an alarm (W_{mn}).

$$C_{op} = W_{op}(pressure) \tag{5.2}$$

Operation cost (C_{op}) can be counted from miscellaneous items. Here we discuss only the one is related to the pressure of the reactor.

$$C_{de} = Q_D \times W_{de} \tag{5.3}$$

Here we use units of production method in counting depreciation. Depreciation (C_{de}) is derived from timing the quantity of production D (Q_D) and depreciation per production D (W_{de}).

$$C_{mt} = \sum Q_i \times W_{mt_i} = Q_A \times W_{mt_A} + Q_B \times W_{mt_B} + Q_C \times W_{mt_C} \tag{5.4}$$

Table 5.1: Factors in calculating PPI

symbol	significance	units
C_{mn}	management cost	\$
C_{op}	operation cost	\$
C_{de}	depreciation	\$
C_{mt}	material cost	\$
R_{sl}	sales revenue	\$
N_{al}	number of alarms	
Q_D	quantity of production D	$kmol$
Q_i	quantity of input A, B, and C	$kmol$
W_{mn}	cost of checking an alarm	$\$/alarm$
W_{op}	function of pressure	\$
W_{de}	depreciation per production D	$\$/kmol$
W_{mt_i}	unit price of input A, B, and C	$\$/kmol$
W_{sl_D}	unit sales price of production D	$\$/kmol$

In computing material cost (C_{mt}), we sum the quantity of input i (Q_i) times its unit price (W_{mt_i}) to get the total amount of material cost.

$$R_{sl} = Q_D \times W_{sl_D} \tag{5.5}$$

Sales revenue (R_{sl}) is the quantity of production D (Q_D) times unit sales price of production D (W_{sl_D}).

Thus PPI is calculated from:

$$PPI = \frac{(C_{mn} + C_{op} + C_{de} + C_{mt})}{R_{sl}} \tag{5.6}$$

From Eq. (5.6), we know PPI is counted by the ratio of costs and revenue. In general, the revenue is always larger than the sum of all costs. This implies $0 \leq$ PPI< 1. Here we assume three cases: high profit (PPI$\simeq$0: revenue is much higher than cost), medium profit (PPI$\simeq$0.5:

cost is about half of revenue), and low profit (PPI$\simeq$1: cost and revenue are about the same) to see the effect of stealthy attacks on different profit product.

Before taking a closer look, we should know that for the following cases, all the stealthy attacks will be stopped before being detected by the mADM, so there is no alarm, which means N_{al}=0. As for $W_{op}(pressure)$ in Eq. (5.2), we don't really go deeply inside to model the characteristic of the operation cost. Here we simply assume $W_{op}(pressure) = 1 + \dfrac{(pressure - 2700)}{300}$ where W_{op} is a constant under steady state pressure (2700kPa) and increasing with pressure before system crashes (3000kPa) (Fig. 5.2). For the high profit case, W_{op} is the function mentioned above. For the medium profit case, W_{op} is 10 times of the function. And W_{op} is 19 times of the function in the low profit case.

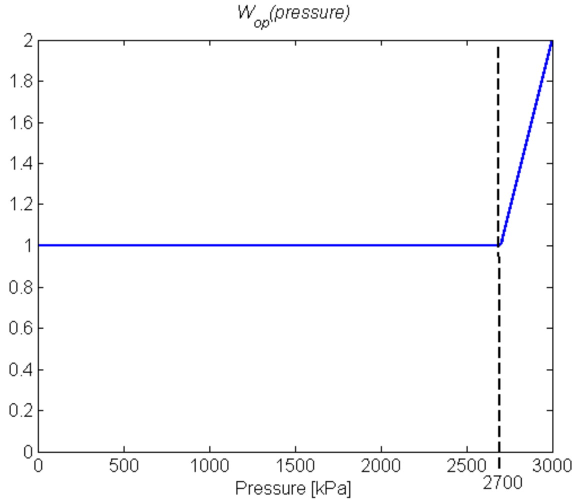

Figure 5.2: Function of pressure

5.2.1 Case 1: High Profit

Assume that W_{mn}=100, W_{de}=0.1, W_{mt_A}=0.2, W_{mt_B}=0.1, W_{mt_C}=0.6, and W_{sl_D}=20 where Rsl is much more larger than the sum of all costs. Running the simulation for 40 hrs with no attack, from Eq. (5.6), we derive a PPI valued 0.0512. Launching the four stealthy attacks mentioned in subsection 4.2.2 to get Fig. 5.3 helps us to understand the effect of stealthy attacks in increasing the PPI.

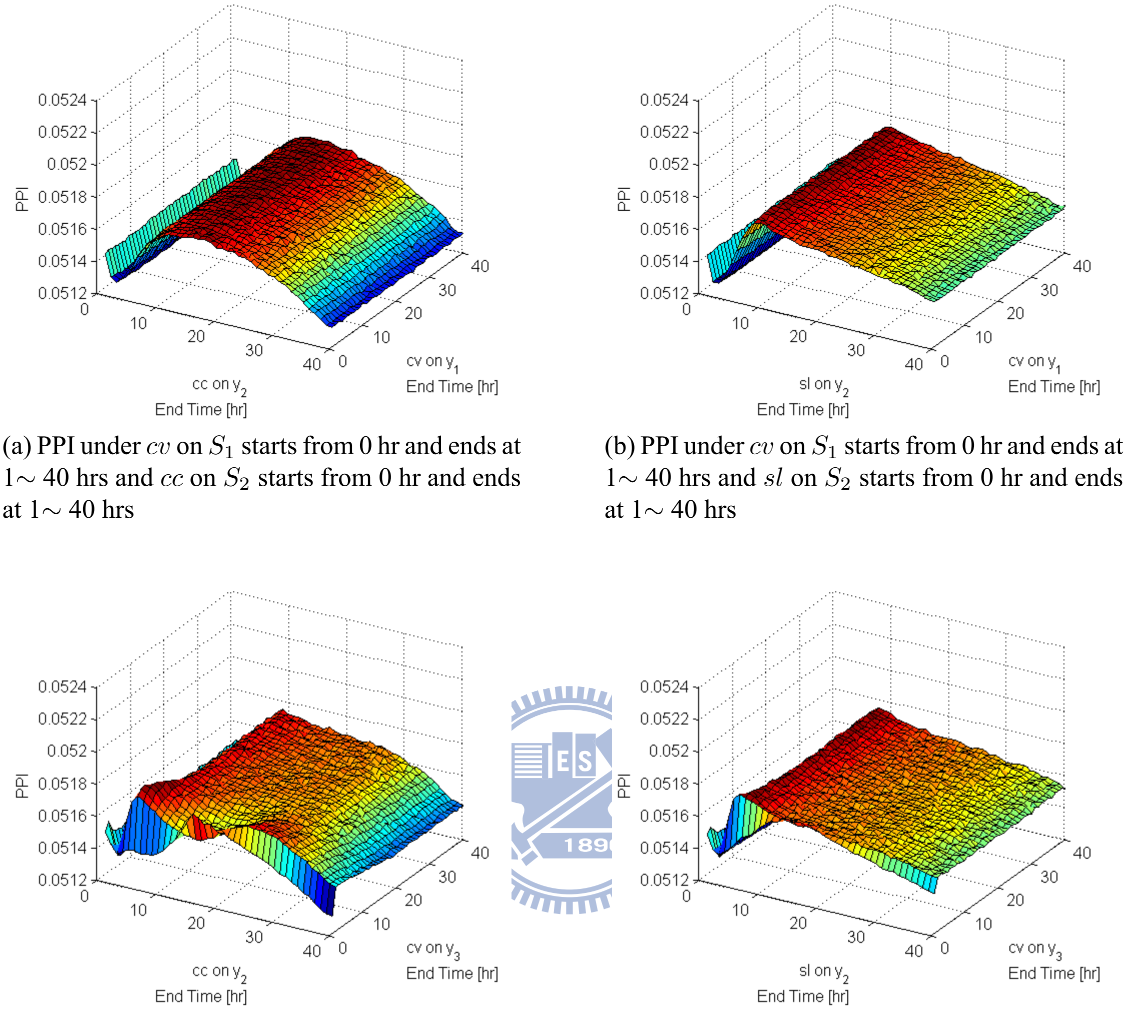

(a) PPI under cv on S_1 starts from 0 hr and ends at 1$\sim$ 40 hrs and cc on S_2 starts from 0 hr and ends at 1$\sim$ 40 hrs

(b) PPI under cv on S_1 starts from 0 hr and ends at 1$\sim$ 40 hrs and sl on S_2 starts from 0 hr and ends at 1$\sim$ 40 hrs

(c) PPI under cv on S_3 starts from 0 hr and ends at 1$\sim$ 40 hrs and cc on S_2 starts from 0 hr and ends at 1$\sim$ 40 hrs

(d) PPI under cv on S_3 starts from 0 hr and ends at 1$\sim$ 40 hrs and sl on S_2 starts from 0 hr and ends at 1$\sim$ 40 hrs

Figure 5.3: high profit

From Fig. 5.3, we get the highest PPI in Fig. 5.3a and Fig. 5.3b are 0.0517 and the highest PPI in Fig. 5.3c and Fig. 5.3d are 0.0518. Comparing to the PPI with no attack (0.0512), there is a very little increase in PPI (1.17%). In other words, if the costs of a \$10,000 product is \$512, it will cost us 6 more dollars under stealthy attacks. The effect of stealthy attacks in increasing PPI is not obvious in a high benefit product.

5.2.2 Case 2: Medium Profit

Assume that W_{mn}=1000, W_{de}=1, W_{mt_A}=2, W_{mt_B}=1, W_{mt_C}=6, and W_{sl_D}=20 where the sum of all costs is about half of Rsl. Running the simulation for 40 hrs with no attack, from Eq. (5.6), we derive a PPI valued 0.5123. By launching the four stealthy attacks mentioned in subsection 4.2.2, we can see the effects of stealthy attacks in increasing PPI from Fig. 5.4.

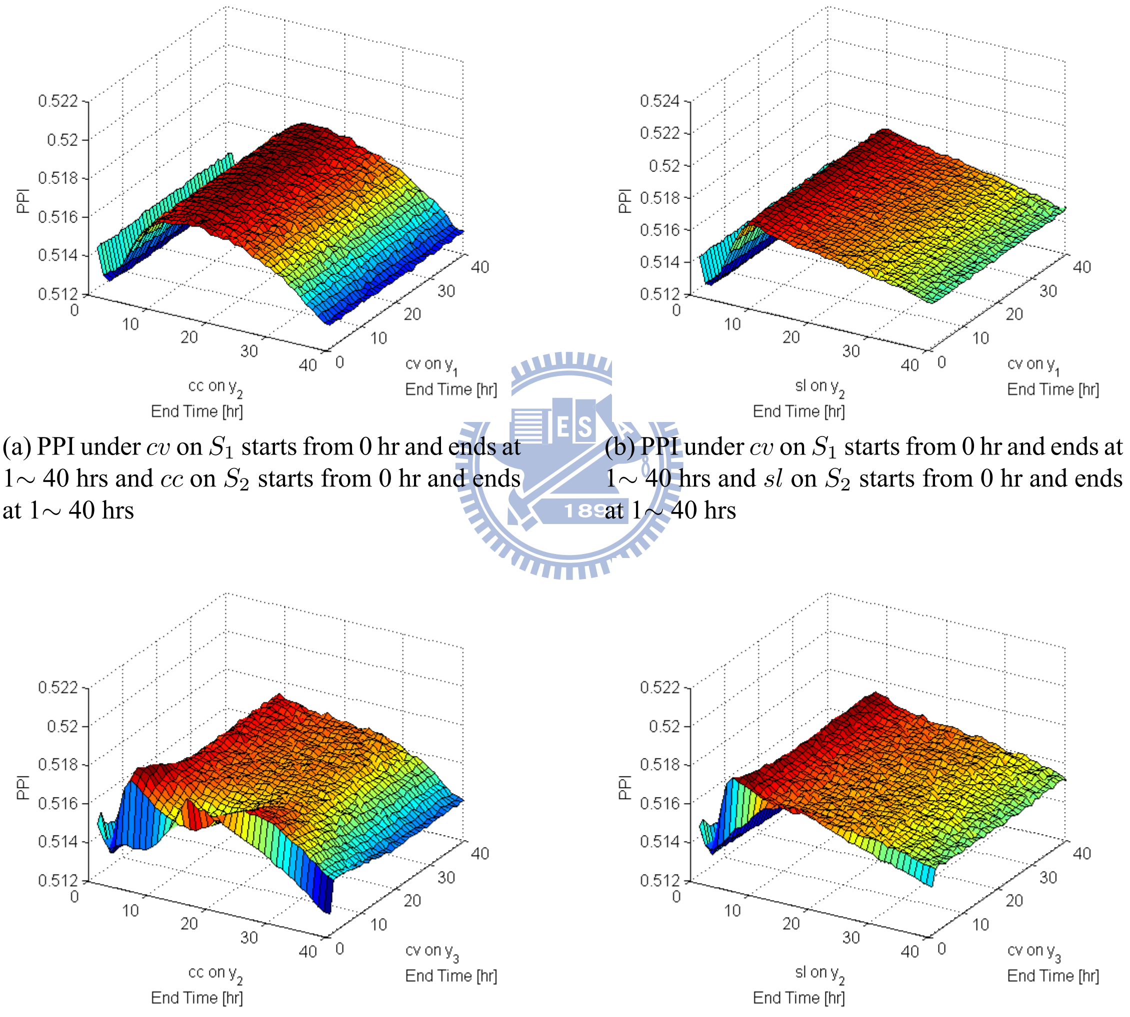

(a) PPI under cv on S_1 starts from 0 hr and ends at 1$\sim$ 40 hrs and cc on S_2 starts from 0 hr and ends at 1$\sim$ 40 hrs

(b) PPI under cv on S_1 starts from 0 hr and ends at 1$\sim$ 40 hrs and sl on S_2 starts from 0 hr and ends at 1$\sim$ 40 hrs

(c) PPI under cv on S_3 starts from 0 hr and ends at 1$\sim$ 40 hrs and cc on S_2 starts from 0 hr and ends at 1$\sim$ 40 hrs

(d) PPI under cv on S_3 starts from 0 hr and ends at 1$\sim$ 40 hrs and sl on S_2 starts from 0 hr and ends at 1$\sim$ 40 hrs

Figure 5.4: medium profit

From Fig. 5.4, we get the highest PPI in Fig. 5.4a, Fig. 5.4b, Fig. 5.4c, and Fig. 5.4d are 0.517, 0.5174, 0.5188, and 5186. To compare with the results in subsection 4.3.2, the higher PPI is positive correlated to the higher pressure can be concluded. But we can see that the increment degree is not as much as in pressure. Though in Fig. 5.4c, cv on S_3 and cc on S_2 can raise the PPI higher than the others, the increment is about only 1.27%.

5.2.3 Case 3: Low Profit

Assume that W_{mn}=1900, W_{de}=1.9, W_{mt_A}=3.8, W_{mt_B}=1.9, W_{mt_C}=11.4, and W_{sl_D}=20 where the sum of all costs is about Rsl. Running the simulation for 40 hrs with no attack, from Eq. (5.6), we can have PPI= 0.973. By launching the four stealthy attacks mentioned in subsection 4.2.2, we can understand the effects of stealthy attacks in increasing PPI from Fig. 5.5.

From Fig. 5.5, we know the highest PPI is Fig. 5.5c $>$ Fig. 5.5d $>$ Fig. 5.5b $>$ Fig. 5.5a. Comparing to the results in subsection 4.3.2, we can also see higher pressure causes higher PPI. Launching stealthy attack lifts the PPI from 0.973 (no attack) to 0.984 (the highest PPI in Fig. 5.5c). There is only 1.13% increment. However, from the view of profit, stealthy attacks can be threatening. For instance, PPI=0.973 can be said as the sum of all costs is \$973 in producing a \$1000 product and by selling it we can earn \$27. After launching stealthy attacks, the sum of all costs rises to \$984 and the earning will be decreased to \$16. Stealthy attacks make about 41% loss in earning. Thus we say low profit case is totally different from high profit case. Stealthy attacks are harmful for low profit product.

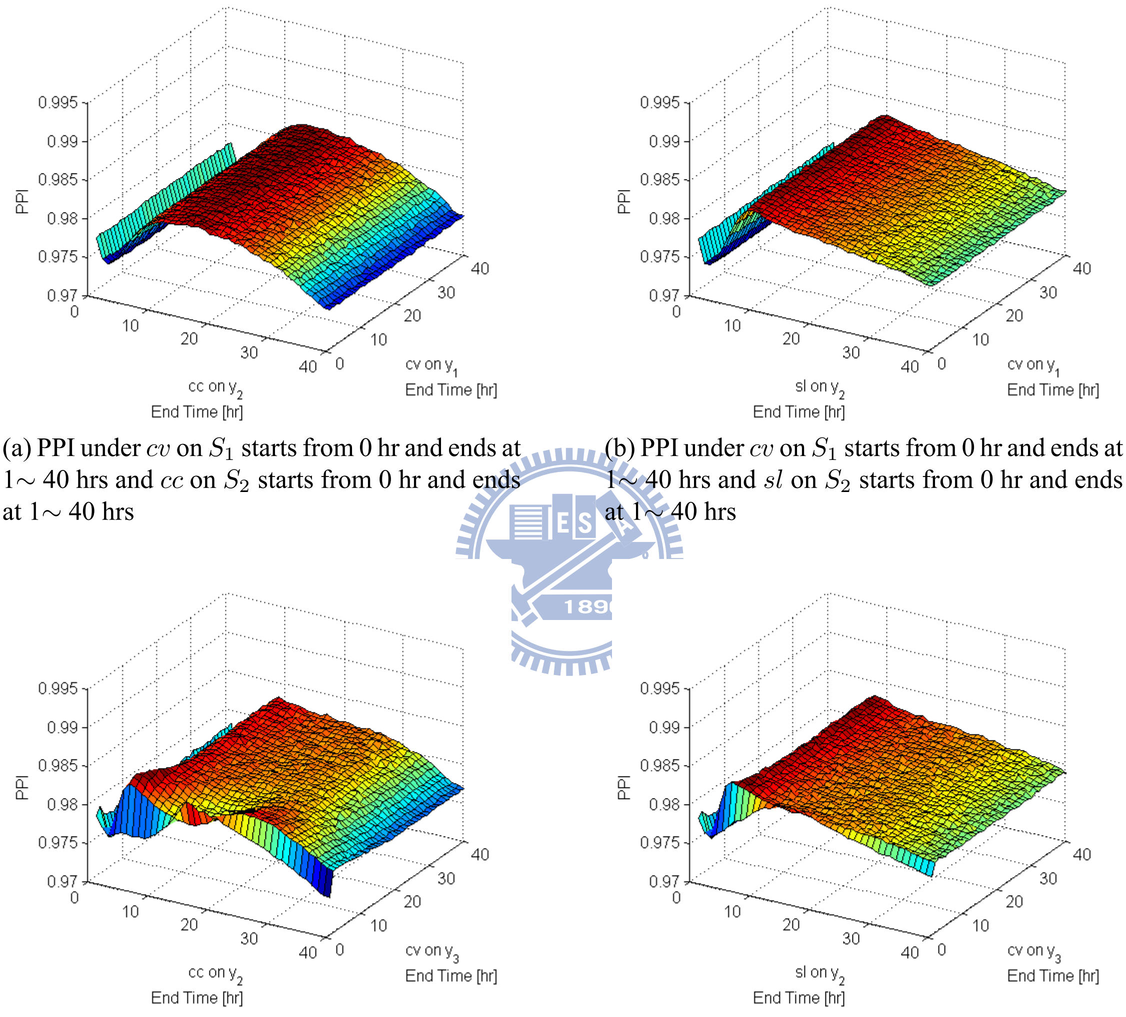

(a) PPI under cv on S_1 starts from 0 hr and ends at 1$\sim$ 40 hrs and cc on S_2 starts from 0 hr and ends at 1$\sim$ 40 hrs

(b) PPI under cv on S_1 starts from 0 hr and ends at 1$\sim$ 40 hrs and sl on S_2 starts from 0 hr and ends at 1$\sim$ 40 hrs

(c) PPI under cv on S_3 starts from 0 hr and ends at 1$\sim$ 40 hrs and cc on S_2 starts from 0 hr and ends at 1$\sim$ 40 hrs

(d) PPI under cv on S_3 starts from 0 hr and ends at 1$\sim$ 40 hrs and sl on S_2 starts from 0 hr and ends at 1$\sim$ 40 hrs

Figure 5.5: Low profit

Chapter 6

Conclusion and Future Work

In this research, we modeled three kinds of stealthy attacks (cv, sl, and cc) to evaluate the parameters-choosing limitation of mADM protecting a well-studied process control system, TE-PCS. By observing the pressure of the reactor, we know the TE-PCS is under the danger of exploding if parameters of mADM are modified over large by an insider. mADM protects the system only at the range where $b = [b_{Lin}, 40b_{Lin})$ and $\tau = (0.2\tau_{Lin}, 1.2\tau_{Lin})$. Otherwise, attacker is likely to launch stealthy attacks to drive the pressure of the reactor over 3000kPa and crash the system.

We also illustrated three case studies to show that stealthy attacks can increase the PPI of the system. From the case studies, we know stealthy attacks have little effect in increasing PPI if the system produces something with high profit. On the other hand if the system produces something with low profit, stealthy attacks decrease the earning enormously.

Even though we have focused on the testing of the mADM for TE-PCS, we believe that our stealthy attacks can be also applied to test any mADM of process control systems possess similar characteristic with the one proposed by Lin et al. . Overall, though our three attack types provide general formats of stealthy attacks, stealthy attacks can be designed more elaborately.

References

[1] A. Daneels and W. Salter, "What Is SCADA?" in *International Conference on Accelerator and Large Experimental Physics Control Systems*, 1999.

[2] Y. Ebata, H. Hayashi, Y. Hasegawa, S. Komatsu, and K. Suzuki, "Development of the Intranet-Based SCADA (Supervisory Control And Data Acquisition System) for Power System," in *Power Engineering Society Winter Meeting, 2000. IEEE*, vol. 3, Jan. 2000, pp. 1656--1661 vol.3.

[3] A. Cardenas, S. Amin, and S. Sastry, "Research Challenges for the Security of Control Systems," in *3rd USENIX Workshop on Hot Topics in Security (HotSec '08). Associated with the 17th USENIX Security Symposium.*, Jul. 2008.

[4] E. Lee, "Cyber Physical Systems: Design Challenges," in *Object Oriented Real-Time Distributed Computing (ISORC), 2008 11th IEEE International Symposium on*, May 2008, pp. 363--369.

[5] A. Cardenas, S. Amin, and S. Sastry, "Secure Control: Towards Survivable Cyber-Physical Systems," in *Distributed Computing Systems Workshops, 2008. ICDCS '08. 28th International Conference on*, Jun. 2008, pp. 495--500.

[6] E. Chikuni and M. Dondo, "Investigating the Security of Electrical Power Systems SCADA," pp. 1--7, Sep. 2007.

[7] E. Byres and J. Lowe, "The Myths and Facts behind Cyber Security Risks for Industrial Control Systems," in *VDE Congress*, 2004.

[8] C.-W. Ten, C.-C. Liu, and G. Manimaran, "Vulnerability Assessment of Cybersecurity for SCADA Systems," vol. 23, no. 4, pp. 1836--1846, Nov. 2008.

[9] A. Creery and E. Byres, "Industrial Cybersecurity for Power System and SCADA Networks," in *Petroleum and Chemical Industry Conference, 2005. Industry Applications Society 52nd Annual*, Sep. 2005, pp. 303--309.

[10] J. Hahn, D. Guillen, and A. T., "Process Control Systems in the Chemical Industry: Safety vs. Security," in *Process Safety Progress*, Mar. 2006.

[11] Z. Lin and Y. Huang, "Threat Assessment and Model-Based Attack Detection for Process Control Systems," Master's thesis, 2009.

[12] J. Downs and E. Vogel, "A Plant-Wide Industrial Process Control Problem," vol. 17, no. 3, pp. 245--255, 1993.

[13] N. Ricker, "Model Predictive Control of a Continuous, Nonlinear, Two-Phase Reactor," vol. 3, pp. 109--109, 1993.

[14] A. Bemporad, D. Mignone, and M. Morari, "Moving horizon estimation for hybrid systems and fault detection," in *American Control Conference, 1999. Proceedings of the 1999*, vol. 4, 1999, pp. 2471--2475 vol.4.

[15] J. Figueiredo and M. Botto, "Automatic Control Strategies Implemented on a Water Canal Prototype," in *International Federation of Automatic Control*, 2005.

[16] A. Dhar and B. Datta, "Optimal Operation of Reservoirs for Downstream Water Quality Control Using Linked Simulation Optimization," vol. 22, no. 6, pp. 842--853, 2008.

[17] Z. Wang, M. Polycarpou, J. Uber, and F. Shang, "Adaptive Control of Water Quality in Water Distribution Networks," vol. 14, no. 1, pp. 149--156, Jan. 2006.

[18] M. Polycarpou, J. Uber, Z. Wang, F. Shang, and M. Brdys, "Feedback Control of Water Quality," vol. 22, no. 3, pp. 68--87, Jun. 2002.

[19] Y. Huang, A. Cardenas, S. Amin, Z. Lin, H. Tsai, and S. Sastry, "Understanding the Physical and Economic Consequencesof Attacks on Control Systems," in *International Journal of Critical Infrastructure Protection*, vol. 2, Oct. 2009, pp. 73--83.

[20] Z. Lin, A. Cardenas, H. Tsai, S. Amin, Y. Huang, and S. Sastry, "Understanding the Physical Consequences of Attacks Against Control Systems," in *International Conference on Critical Infrastructure Protection*, Mar. 2009.

[21] ------, "Security Analysis for Process Control Systems," in *ACM Conference on Computer and Communications Security*, Nov. 2009.